

The Fundamental Diagram and the Statistics of a Passageway

Guillermo A. Frank* Ignacio M. Sticco[†] Fernando E. Cornes[‡]
 Claudio O. Dorso[§]

Abstract

The (qualitative) relation between pedestrian flow and density has been shown to follow a common pattern on multiple real life situations. This pattern distinguishes between a free-flow regime (for low densities) and a congested regime (for high densities). However, theoretical models, such as the Social Force Model (SFM), can handle this behavior if the right friction (or the pedestrian relaxation time) is set. We carried out statistical and numerical tests in order to match our SFM simulations with experimental data on the Jamarat bridge (pedestrians walking along a straight corridor). We concluded that fittings should not care on the friction (or the pedestrian relaxation time) itself, but on other "reduced" parameters with fewer degrees of freedom.

Key Words: Panic, contagion

1. Introduction

Researchers postulated that either the environment and the individuals' own desire affect the pedestrians motion in a similar way as forces do with respect to the momentum of particles (Helbing 2000; Helbing 1995). This "social force model" (SFM) nicely bridged the socio-psychological phenomenon of crowds behavior to the "microscopic" formalism of moving particles. The model succeeded at this instance to explain why the crowd evacuation slows down as pedestrians try harder to escape from a dangerous situation (*i.e.* "faster is slower" effect) (Helbing 2000; Parisi, 2005; Parisi, 2007).

Some questioning arose on the true psychological tendency of the pedestrians to stay away from each other. While the social forces accomplish this tendency, it attains a somewhat unrealistic "colliding behavior" for slowly moving pedestrians (Lakoba, 2005). His (her) repulsive tendency is expected to decrease as approaching a more crowded environment. The small fall-off length $B = 0.08$ m suggested by Helbing (2000) does not completely solve this issue. It neither agrees with the fact that pedestrians prefer to keep a comfortable 0.5 m distance between each other in a moderately crowded environment, nor it fits accurately the empirical velocities reported for non-panicking crowds (Lakoba, 2005).

Researchers turned back to examine the available data on the velocity and flux behavior for different density environments (Helbing, 2007; Seyfried, 2005; Seyfried, 2008). Helbing (2007) is a wonderful summary of empirical data from literature, and their own data set, acquired from videos of the Muslim pilgrimage in Mina-Makkah (2006). They showed from the empirical fundamental diagram (flux J versus density ρ) that highly dense crowds

*Unidad de Investigación y Desarrollo de las Ingenierías, Universidad Tecnológica Nacional, Facultad Regional Buenos Aires, Av. Medrano 951, 1179 Buenos Aires, Argentina

[†]Departamento de Física, Facultad de Ciencias Exactas y Naturales, Universidad de Buenos Aires, Pabellón I, Ciudad Universitaria, 1428 Buenos Aires, Argentina

[‡]Departamento de Física, Facultad de Ciencias Exactas y Naturales, Universidad de Buenos Aires, Pabellón I, Ciudad Universitaria, 1428 Buenos Aires, Argentina

[§]Instituto de Física de Buenos Aires, Pabellón I, Ciudad Universitaria, 1428 Buenos Aires, Argentina.

(seemingly up to 10 p/m^2) do not drive the pedestrians velocity to zero, although the reasons for this remain rather obscure.

The high density regime appears to be the most cumbersome one. Caution was claimed when (automatically) transferring the usual “calibrated” parameters of the SFM to this regime. It was argued that the pedestrians’ body size distribution and the “situational context” are somewhat responsible for the unexpected departure from these parameters (Johansson, 2007; Kwak, 2017). But other researchers pointed out that this departure actually expresses the lack of a mechanism to properly handle the pedestrians’ “required space to move”. Some modifications to the basic SFM were then proposed to overcome this difficulty (Parisi, 2009; Seyfried, 2006).

Although a mechanism allowing an “increase of the space to move” (due to the fear of crushing or injury) is a compelling necessity in the context of the SFM, a sharp “re-calibration” of the model for high density situations appears not to be completely satisfactory (Johansson, 2009). A more “natural” way of handling this matter requires a deep examination of the current SFM parameters. The net-time headway (roughly, the relaxation time) was first examined in Johansson (2009). The author sustains the hypothesis that the pedestrians net-time headway should increase until there is “enough space to make a step”. He shows that a density dependent net-time headway is a suitable parameter to smartly reproduce the empirical fundamental diagram for highly dense crowds (Johansson, 2009).

Our own examination of the SFM parameters suggests that not only the net-time headway, but the friction between pedestrians (and with the walls) can reproduce the pattern of the fundamental diagram. Our working hypothesis is that friction is the crucial parameter in the dynamics of highly dense crowds. We actually sustain the SFM model with no further “re-calibrations”, but with the right friction setting, in order to meet the fundamental diagram pattern.

We want to emphasize that although the friction setting appearing in Helbing (2000) is a commonly accepted estimate throughout the literature, other values have also been proposed (Colombi, 2017). We intend our setting, however, as an experimental based parameter, suitable for high dense crowds.

The investigation is organized as follows. We first recall the SFM in Section 2.1, while including the precise definitions for flux, density and clustered structures. Section 3 presents our numerical simulations for pedestrians moving through corridors. The corresponding results are shown in Section 4. Our main conclusions are detailed in the closing Section 5. A complementary simple model for pedestrians moving through a corridor has been included in the Appendix.

2.

2.1 The Social Force Model

The Social Force model states that human motion is caused by the desire of people to reach a certain destination, as well as other environmental factors. The pedestrians behavioral pattern in a crowded environment can be modeled by three kind of forces: the “desire force”, the “social force” and the “granular force”.

The “desire force” represents the pedestrian’s own desire to reach a specific target position at a desired velocity v_d . But, in order to reach the desired target, he (she) needs to accelerate (decelerate) from his (her) current velocity $\mathbf{v}^{(i)}(t)$. This acceleration (or deceleration) represents a “desire force” since it is motivated by his (her) own willingness. The corresponding expression for this forces is

$$\mathbf{f}_d^{(i)}(t) = m_i \frac{v_d^{(i)} \mathbf{e}_d^{(i)}(t) - \mathbf{v}^{(i)}(t)}{\tau} \quad (1)$$

where m_i is the mass of the pedestrian i . \mathbf{e}_d corresponds to the unit vector pointing to the target position and τ is a constant related to the relaxation time needed to reach his (her) desired velocity. For simplicity, we assume that v_d remains constant during the entire process and is the same for all individuals, but \mathbf{e}_d changes according to the current position of the pedestrian. Detailed values for m_i and τ can be found in Frank (2011).

The “social force” represents the psychological tendency of any two pedestrians, say i and j , to stay away from each other. It is represented by a repulsive interaction force

$$\mathbf{f}_s^{(ij)} = A_i e^{(R_{ij}-r_{ij})/B_i} \mathbf{n}_{ij} \quad (2)$$

where (ij) means any pedestrian-pedestrian pair, or pedestrian-wall pair. A_i and B_i are fixed values, r_{ij} is the distance between the center of mass of the pedestrians i and j and the distance $R_{ij} = R_i + R_j$ is the sum of the pedestrians radius. \mathbf{n}_{ij} means the unit vector in the $\vec{j}i$ direction.

Any two pedestrians touch each other if their distance r_{ij} is smaller than R_{ij} . Analogously, any pedestrian touches a wall if his (her) distance r_{ij} to the wall is smaller than R_i . In these cases, an additional force is included in the model, called the “granular force”(i.e. friction force). This force is considered to be a linear function of the relative (tangential) velocities of the contacting individuals. In the case of the friction exerted by the wall, the force is a linear function of the pedestrian tangential velocity. Its mathematical expression reads

$$\mathbf{f}_g^{(ij)} = \kappa (R_{ij} - r_{ij}) \Theta(R_{ij} - r_{ij}) \Delta \mathbf{v}^{(ij)} \cdot \mathbf{t}_{ij} \quad (3)$$

where κ is the friction coefficient. The function $\Theta(R_{ij} - r_{ij})$ is zero when its argument is negative (that is, $R_{ij} < r_{ij}$) and equals unity for any other case (Heaviside function). $\Delta \mathbf{v}^{(ij)} \cdot \mathbf{t}_{ij}$ represents the difference between the tangential velocities of the sliding bodies (or between the individual and the walls).

The above forces actuate on the pedestrians dynamics by changing his (her) current velocity. The equation of motion for pedestrian i reads

$$m_i \frac{d\mathbf{v}^{(i)}}{dt} = \mathbf{f}_d^{(i)} + \sum_{j=1}^N \mathbf{f}_s^{(ij)} + \sum_{j=1}^N \mathbf{f}_g^{(ij)} \quad (4)$$

where the subscript j represents all the other pedestrians (excluding i).

In the original model, there is no distinction between the friction coefficient of pedestrian-pedestrian interaction and pedestrian-wall interaction. Both interactions are modeled with the same constant parameter κ . In this paper we analyze situations in which the friction

coefficient may take different values. We define κ_i and κ_w as the friction coefficient related to the pedestrian-pedestrian interaction and the pedestrian-wall interaction, respectively.

2.2 Fundamental Diagram

We follow the same definition as in Helbing (2007) regarded to the fundamental diagram analysis. That is, we mean by the local density at place $\vec{r} = (x, y)$ and time t the following expression

$$\rho(\vec{r}, t) = \sum_j f(\vec{r}_j(t) - \vec{r}) \quad (5)$$

where function $f(\vec{r}_j(t) - \vec{r})$ is a Gaussian distance-dependent weight function defined as

$$f(\vec{r}_j - \vec{r}) = \frac{1}{\pi R^2} \exp[-\|\vec{r}_j - \vec{r}\|^2 / R^2] \quad (6)$$

$\vec{r}_j(t)$ are the positions of the pedestrians j in the surroundings of \vec{r} and R is a measurement parameter. The local speeds are defined as the weighted average

$$\vec{V}(\vec{r}, t) = \frac{\sum_j \vec{v}_j f(\vec{r}_j(t) - \vec{r})}{\sum_j f(\vec{r}_j(t) - \vec{r})} \quad (7)$$

while flow is determined according to the fluid-dynamic formula

$$\vec{J}(\vec{r}, t) = \rho(\vec{r}, t) \vec{V}(\vec{r}, t) \quad (8)$$

2.3 Clustering structures

A characteristic feature of pedestrian dynamics is the formation of clusters. Clusters of pedestrians can be defined as the set of individuals that for any member of the group (say, i) there exists at least another member belonging to the same group (j) in contact with the former. Thus, we define a ‘‘granular cluster’’ (C_g) following the mathematical formula given in Parisi (2005)

$$C_g : P_i \in C_g \Leftrightarrow \exists j \in C_g / r_{ij} < (R_i + R_j) \quad (9)$$

where (P_i) indicate the i th pedestrian and R_i is his (her) radius (shoulders width). That means, C_g is a set of pedestrians that interact not only with the social and the desired forces, but also with granular forces (*i.e.* friction forces). The size of the cluster is defined as the number of pedestrians belonging to it. The fraction of clustered individuals is defined as the ratio between clustered individuals with respect to the total number of individuals in the crowd.

3. Simulations

The simulations process were performed on a straight corridor of length $L = 28$ m (with periodic boundary conditions) and variable width w . We explored widths ranging from $w = 2$ m to $w = 40$ m. The corridor had two side walls, placed at $y = 0$ and $y = w$, respectively. The length of each wall was L . The pedestrians were modeled as soft spheres of radius $R_i = 0.23$ m. Initially, the individuals were randomly distributed along the corridor with a fixed global density (p/m^2) and with random initial velocities, resembling a Gaussian distribution with null mean value. We explored global density values in the range

$1 \text{ p m}^{-2} < \rho < 9 \text{ p m}^{-2}$. The number of pedestrians in the simulation was given by the global density and the corridor dimensions chosen in each case.

The simulations were supported by LAMMPS molecular dynamics simulator with parallel computing capabilities (Plimpton, 1995). The time integration algorithm followed the velocity Verlet scheme with a time step of 10^{-4} s. All the necessary parameters were set to the same values as in previous works (see Sticco, 2017, except for the friction coefficient κ . In this work we use the common value $\kappa = 2.4 \times 10^5 \text{ Kg m}^{-1} \text{ s}^{-1}$, but we eventually set the newly defined parameters $\kappa_i = 2.4 \times 10^6 \text{ Kg m}^{-1} \text{ s}^{-1}$ and $\kappa_w = 2.4 \times 10^6 \text{ Kg m}^{-1} \text{ s}^{-1}$, being κ_i and κ_w the pedestrian-pedestrian friction coefficient and the pedestrian-wall friction coefficient, respectively.

We implemented special modules in C++ for upgrading the LAMMPS capabilities to attain the social force model simulations. We also checked over the LAMMPS output with previous computations (see Parisi 2005, 2007; Frank 2011, 2015, 2016).

The desired velocity for each pedestrian i was $\vec{v}_d^{(i)} = 1 \text{ m/s } \hat{e}_d^{(i)}$, where the target $\hat{e}_d^{(i)}$ was set as $\hat{e}_d^{(i)} = (L, y_i) / \|(L, y_i)\|^{-1}$, being L the x -location of the end at the corridor and y_i the y -location corresponding to the i th pedestrian (see Fig. 8). This allowed the pedestrians to move from left to right in an unidirectional flow. Pedestrians that surpassed $x = L$ were re-injected at $x = 0$, preserving their current velocity and y -location (*i.e.* periodic boundary conditions). This mechanism was carried out in order to keep the crowd size unchanged.

The measurements were taken once the system reached the stationary state ($t = 30$ s), while the configurations of the systems were recorded every 0.05 s, that is, at intervals as short as 10% of the pedestrians relaxation time (see Sec. 2.1). The recorded magnitudes were the pedestrians positions and velocities for each process. We also computed the clustering structures using a LAMMPS built in function.

We warn the reader that, for simplicity, we will not include the units corresponding to the numerical results. Remember that the friction coefficient has units $[\kappa] = \text{Kg m}^{-1} \text{ s}^{-1}$, the density $[\rho] = \text{p m}^{-2}$ and the flow $[J] = \text{p m}^{-1} \text{ s}^{-1}$.

4. Results

4.1 Fundamental diagram in the original model

In this Section we present the results relating the local flow, velocity and density (*i.e.* the fundamental diagram). The measurements were taken in the middle of the corridor using the definitions given in Eq. (7) and Eq. (8), and as shown in Fig. 1. All the results shown here correspond to $R = 1$ m (see Eq. (8) and Fig. 1). We further varied R until $R = 3$, but no significant changes were observed.

Fig 2, shows the fundamental diagram (flow vs. density) for different corridor widths. We can distinguish the two typical regimes of the fundamental diagram. In the free flow regime ($\rho < 5$), the flow increases linearly with the density, since collisions between pedestrians are scarce. Pedestrians are able to achieve their desired velocity, leading to a flow that grows linearly with the density ($J \sim \rho$) until $\rho = 5$. This behavior applies to all the analyzed corridor widths.

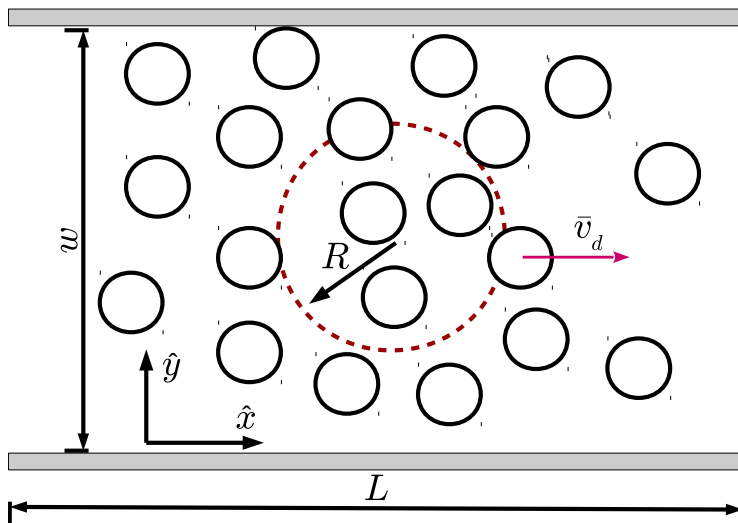


Figure 1: Schematic diagram for individuals in the corridor. The circles represent pedestrians moving from left to right. w represents the corridor width, L represents the length. The rectangular boxes are upper and lower blocks that represent the walls of the corridor. The dashed circle in the middle corresponds to the measurement region and R is the measurement parameter from Eq. (8)

On the other hand, we have the congested branch for $\rho > 5$. Here we face two different scenarios:

- (i) For narrow corridors (say $w < 10$) we can see that the flow reduces as the density increases. This resembles the traditional behavior of the fundamental diagram reported in the literature.
- (ii) For wide corridors (say $w > 15$) we see that the flow increases with density. This contradicts the typical behavior of the fundamental diagram.

In the case of narrow corridors, both the simulated case and the empirical results converge to a constant flow value. It is remarkable that the system does not reach a freezing state such as the one reported in Kwak (2017). Recall that our simulations do not include any respect factor (see Parisi, 2009), or changes in the net-time headway (Helbing, 2007), or the urge to see an attraction (Kwak, 2017). We assume a well defined target and the same v_d for all the pedestrians.

The inset in Fig. 2 corresponds to the empirical data from Helbing (2007). at the entrance of the Jamarat bridge (the corridor width was $w = 22$ m). Notice that our simulated results corresponding to a $w = 22$ m corridor, exhibit a different behavior along the congested regime. In the simulated case, the flow increases even for the greatest explored density. On the contrary, the empirical data exhibit a flow reduction for $\rho > 5$ until reaching a plateau for the highest explored density values.

In order to fulfill the experimental fundamental diagram, it becomes necessary that the flow at the maximum explored density ($\rho_{max} = 9$) does not exceed the flow at $\rho = 5$ (upper bound). That is: $J(\rho = 9) < J(\rho = 5)$. From the flow definition in Eq. (8) we can derive the bounding values

$$v(\rho_{max}) < \frac{5v_d}{\rho_{max}} \leq \frac{5}{9}v_d \quad (10)$$

As our desired velocity is fixed at $v_d = 1$ m/s, we conclude that the speed at the maximum density has to be bounded by $v(\rho_{max}) \leq 0.5$ m/s in order to satisfy the qualitative behavior of the (experimental) fundamental diagram reported in the literature.

The above reasoning is consistent with the speed-density results shown in Fig. 3. As a visual guide we plotted $v = 0.5$ m/s with a horizontal dashed line. The close examination of $\rho_{max} = 9$ shows that values corresponding to the wide corridors ($w = 15$ m and $w = 22$ m) exceed $v = 0.5$ m/s. But, those values corresponding to narrow corridors fall below $v = 0.5$ m/s.

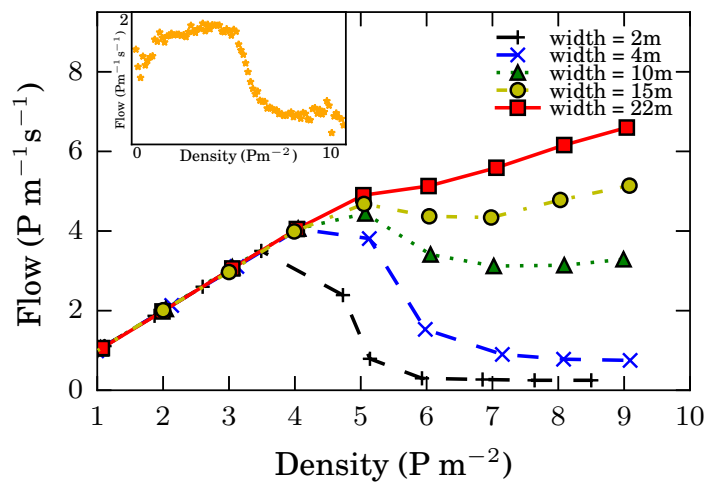


Figure 2: Flow (J) as a function of the density (ρ) for different widths. Initially, pedestrians were randomly distributed along the corridor. The measurements were taken in the middle of the corridor once the system reached the stationary state (see Fig. 1). The length of the corridor was $L = 28$ m for all cases (with periodic boundary conditions in the x direction).

The results shown in Fig. 3 confirm the fact that when the density is low enough, pedestrians manage to walk at the desired velocity ($v = v_d = 1$ m/s). Above $\rho > 5$, however the velocity begins to slow down. The inset shows the experimental data at the entrance of the Jamarat bridge. We may conclude that our simulations agree with the experimental data for narrow corridors, but disagree as these become wider. The wider the corridor, the greater the velocity for all the density values. In Section 4.2 we will further discuss this topic.

It should be pointed out that the Jamarat data does not exhibit a “really” constant velocity for low densities. But this seems reasonable since our simulations do not include the complexities of the real situation when the density is low. We will not analyze this phenomenon in this investigation.

We may summarize our first results as follows. We were able to validate the seminal SFM for narrow corridors through the fundamental diagram. However, the SFM (in its current version) disagrees with experimental data as the corridors widen. We will focus in

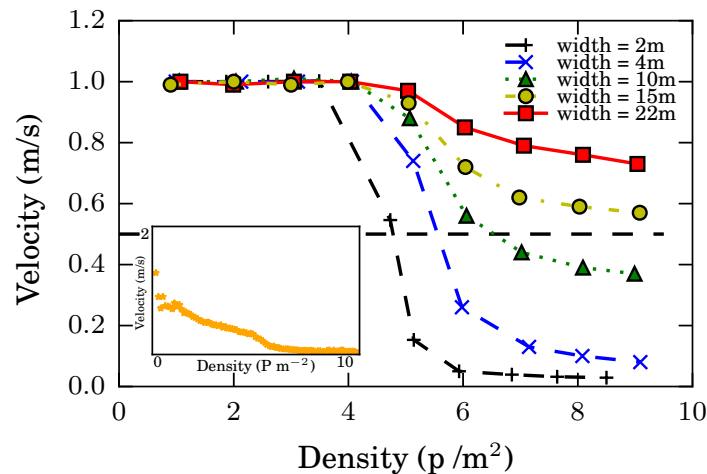


Figure 3: Mean speed (V) as a function of the density (ρ) for different widths. Initially, pedestrians were randomly distributed along the corridor. The measurements were taken in the middle of the corridor once the system reached the stationary state (see Fig.1). The length of the corridor was 28 m in all cases (with periodic boundary conditions in the x direction).

the next Section on the velocity profile in order to investigate this discrepancy.

4.2 Velocity profile

As we mentioned in Section 4.1, when the density is low, pedestrians achieve the desired velocity ($v = v_d = 1$ m/s). Since the results of the previous Section only hold for the area located in the middle of the corridor (see Fig.1), we want to shed some light and understand what is happening across the entire corridor.

Fig. 4 shows the velocity profile (velocity vs. y -location) of the pedestrians across the corridor (see caption for details). We can see that low-density situations lead to a cruising velocity profile $v = v_d$. This is valid for every location in the corridor (not only the center as was previously noticed in Section 4.1). For higher densities, the velocity profile turns into a parabola-like function. This shape resembles the usual velocity profile for laminar flow in a viscous fluid, where the velocity increases toward the center of a tube. In our case, pedestrians near the walls are the ones with the lower velocity. The velocity increases when departing from the wall until it reaches the maximum at the center of the corridor. This behavior suggests that the wall friction on the pedestrians, is playing a relevant role on the velocity distribution. We did some tests removing the walls, while setting periodic boundary conditions in the y -coordinate. This yield to constant-cruising velocity profiles for all the densities, confirming that the walls are a necessary condition for attaining a parabola-shaped speed profile.

Fig. 5 shows the velocity profile for different widths. The horizontal axis of the plot corresponds to the y -location normalized by the width of the corridor. The density chosen was $\rho = 6$ since we wanted to study a situation in which pedestrians slow down. Recall that when $\rho < 5$, collisions between pedestrians are not relevant (within the SFM). We can see that the lowest velocities occur in the regions near the walls. Additionally, there is a clear relation between v_{max} and the corridor width. That is, the wider the corridor, the higher

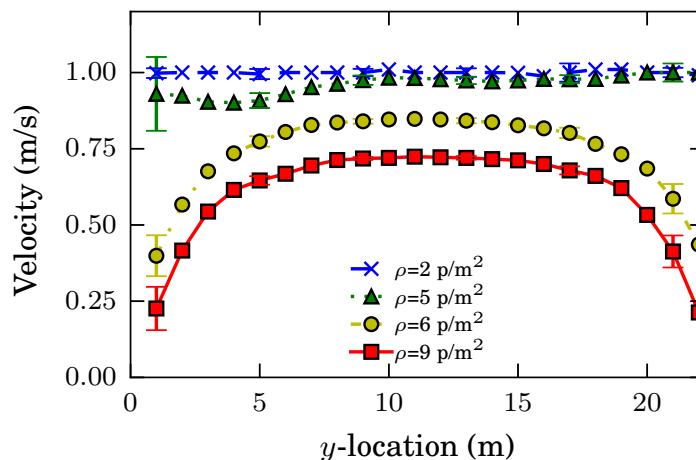


Figure 4: Mean velocity profile (velocity vs y -position) for different densities (see the inserted legend). The simulated corridor was 28 m length. Pedestrians walk from left to right with periodic boundary condition in the x -direction. Initially, pedestrians were randomly distributed, the corridor width was $w = 22$ m for all the cases. The bin size was 1 m.

the maximum reached velocity.

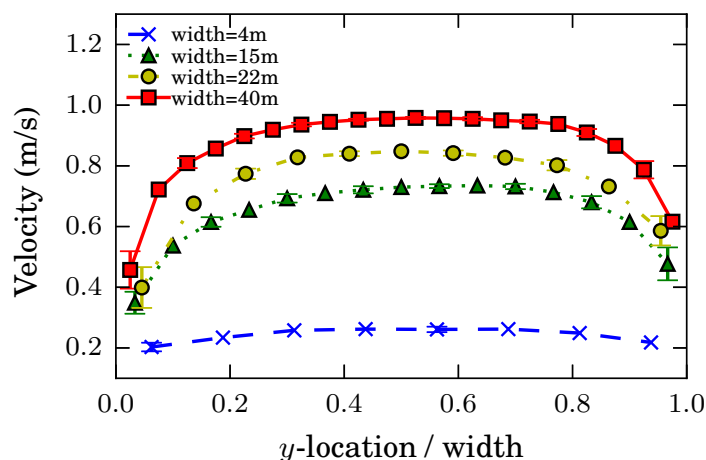


Figure 5: Velocity profile (velocity vs y -position) for different corridors width (see legend for the corresponding widths). The simulated corridor was 28 m length. Pedestrians walk from left to right with periodic boundary condition in the x -direction. Initially, pedestrians were randomly distributed, the density was $\rho = 6$ in all the cases (high density regime). The bin size was 1 m except for $w = 4$ m since the bin was 0.5 m.

Fig. 6 exhibits the scaled velocity profile. The horizontal axis is normalized by the corresponding corridor width (just like in Fig. 5). Now, the vertical axis is normalized by the maximum velocity (v_{max}) corresponding to each data set. Filled markers correspond density $\rho = 9$, while empty markers correspond to $\rho = 6$. Notice that all the data follow the same pattern, suggesting that the velocity profile exhibits a somewhat fundamental behavior, regardless the scale of the corridor (and the density). Hence, the velocity growth

rate from the wall towards the center of the corridor, is the same in spite of the size of the corridor width.

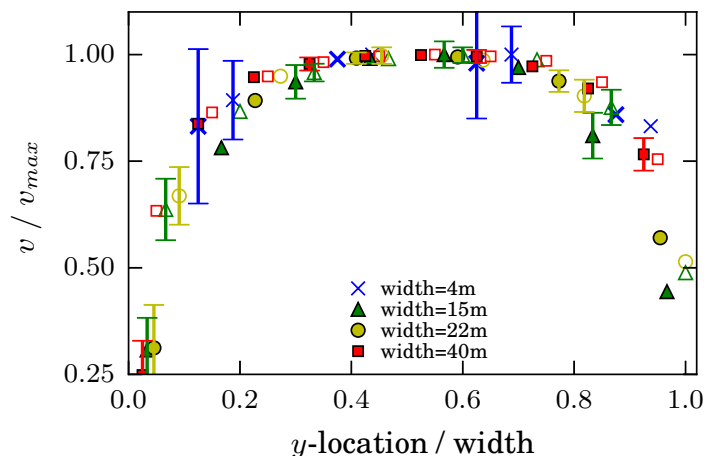


Figure 6: Scaled velocity profile (normalized velocity) vs. y -location for different corridors width (see legend for the corresponding widths) and two different densities. Empty markers correspond to $\rho = 6$ while filled markers correspond to $\rho = 9$. The simulated corridor was 28 m length. Pedestrians walk from left to right with periodic boundary condition in the x -direction. Initially, pedestrians were randomly distributed. The horizontal axis is normalized by the corridor width, the vertical axis is normalized by the maximum velocity reached in each case. The bin size was 1 m for all cases except for $w = 4$ m since the bin was 0.5 m.

In summary, the scaled velocity profile does not report any relevant different as the corridor widens (withing the high density regime). This suggests that the pedestrian dynamics remain essentially the same. The maximum attainable velocity (v_{max}), however, seems to be a sensible parameter with respect to the flux. The narrow corridors attain lower values of v_{max} and thus lower flux. We may expect the flow not to increase if v_{max} remains low enough along the explore density range.

In this subsection we have shown that the velocity profile has a parabola shape. Pedestrians attain the maximum velocity in the middle of the corridor while the minimum is by the walls. We found out that once normalized by v_{max} and the corridor width, the velocity profile yields a universal behavior (regardless the width of the corridor).

We may hypothesize that the friction force is somehow the key factor in the flow reduction, as reported in the experimental fundamental diagram. This hypothesis further inspired us to analyze the role of the friction coefficient in a simple model for the corridor (see Appendix).

4.3 Friction modification

The results shown so far indicate that friction may be the key magnitude for fitting the fundamental diagram into the experimental data. We want to make clear that fitting the experimental data means mimicking (qualitatively) the congested regime reported by different authors for corridors as width as 22 m. The seminal version of the Social Force Model proposes the same friction coefficient for the pedestrian-pedestrian interaction and

the pedestrian-wall interaction. The proposed value was $\kappa = 2.4 \times 10^5$. This value is widely used in many studies despite it lacks a rigorous foundation.

We tested the friction coefficient modification in Appendix 7 and we found that the fundamental diagram experiences a qualitatively change when the friction coefficient κ is varied. We further performed numerical simulations in the context of the SFM. We call κ_i as the friction coefficient of the pedestrian-pedestrian interaction and κ_w as the friction coefficient of the pedestrian-wall interaction. Fig. 7 shows the flow vs density for different values of κ_i and κ_w .

The triangular symbols in Fig. 7 corresponds to the increase in one order of magnitude of the wall friction (now $\kappa_w = 2.4 \times 10^6$), leaving the pedestrian-pedestrian friction unchanged (*i.e.*, $\kappa_i = 2.4 \times 10^5$). We can see that the flow reduces a little bit, but this is not enough to change significantly the congested regime.

The circles in Fig. 7 correspond to a modification of the friction between pedestrians without changing the value of the wall friction. We increased the pedestrian-pedestrian friction by a factor of ten ($\kappa_i = 2.4 \times 10^6$). Here we see a significant reduction of the flow. The qualitative behavior resembles the fundamental diagram reported by Helbing *et al.* with a well defined congested regime for the greatest densities.

We also tested the case were both friction coefficients surpass ten times the value of the original model (now $\kappa_w = \kappa_i = 2.4 \times 10^6$). The squared symbols represent this scenario. As expected, the flow reduces significantly respect the original case (cross symbol). Interestingly, the reduction of the flow is more than the reduction due to the increment of κ_i plus the reduction of the flow due to κ_w . This behavior is indicative that the superposition principle does not hold in this system because of the non-linearity of the equation of motion.

This finding allows us to affirm that the friction plays a crucial role in the functional behavior of the fundamental diagram. The increment of both individual-individual friction and wall friction are determinant in order to achieve a congested regime. More specifically, the empirical behavior for the fundamental diagram can be achieved by properly increasing the friction coefficients.

Recall that other authors address the “congested regime problem” by modifying different aspects of the model. Parisi (2009) imposes zero desired velocity once pedestrians are close enough, Johansson (2009) increases the relaxation time in order to slow down the net-time headway, and more recently, Kwak (2017) induce the jamming transition by an attraction. Many of these approaches seem to be equivalent. In Appendix 6 we discuss about how the modification of the relaxation time and the increment of the friction coefficient yield a similar effect, since both affect the same term in the reduced-in-units equation of motion.

We claim that in real scenarios, a combination of all these factors may be the cause of the marked flow reduction that portray the fundamental diagram. The pedestrians path can be very complex even if it is a simple enclosure (straight corridor) and the target is well defined (unidirectional flow). Beyond the complexities given by the internal motivations of pedestrians, we strongly suggest studying and modeling coefficients of friction between individuals and the friction with the walls. These two parameters have shown to be very important in the pedestrian dynamics and deserve a closer inspection in future research.

We want to emphasize that the proposals stated by Parisi (2009), Johansson (2009) and Kwak (2017) only apply under normal conditions. If a crowd is under high levels of anxiety (*i.e.* panic), pedestrians will neither keep distance between each other, nor will feel the urge to see an “attraction”. The only goal in an evacuation under panic is to leave the room. Thus, studying the friction coefficients may be a critical factor to properly reproduce the dynamics of a massive evacuation under stress.

With all these insights, we can say that the narrow corridors have no drawback in the fitting of the flow vs. density relation because very high velocities are not attainable. This happens because in narrow corridors, the friction of the walls has a lot of “relative weight” in the overall friction of the system. The friction exerted by the walls is fundamental in order to produce the parabolic shape of the velocity profile. The walls provide friction force in the opposite direction to the speed of the individual (drag backwards), since they act like a fixed pedestrian. In other ways, friction between pedestrians can produce either drag forward or drag backwards depending on the the contacting pedestrians velocities (see Eq. 3).

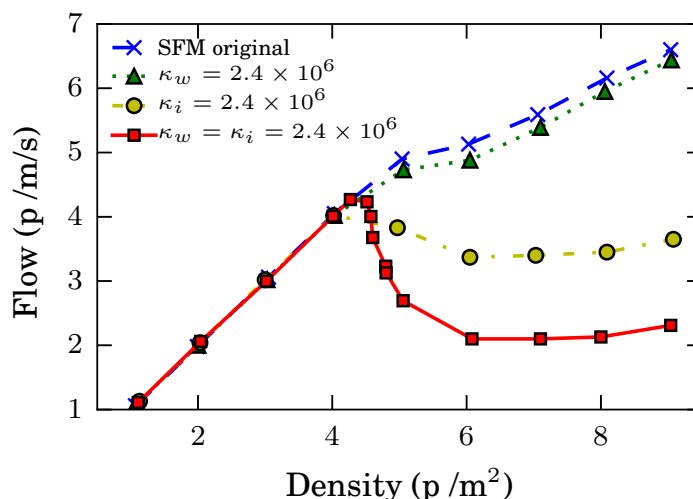


Figure 7: Fundamental diagram (flow vs density) for different friction coefficient (see legend for the corresponding values). The simulated corridor was 28 m length. Pedestrians walk from left to right with periodic boundary condition in the x -direction. Initially, pedestrians were randomly distributed. For each density, we measure the flow once the system reaches the stationary state.

In this subsection we have shown that an adequate modification of the friction coefficients yields a fundamental diagram that follows qualitatively the behavior reported through empirical data (say flow reduction for the highest densities). We have also discussed different approaches proposed by other authors in order to overcome this problem. See Appendix 6 for a more detailed discussion.

5. Conclusions

Our investigation focused on the fundamental diagram in the context of the social force model. We compared empirical data recorded at the entrance to the Jamarat bridge (see Helbing, 2007) with our own SFM simulations. We found out that the social force model in its original version does not fit into the empirical fundamental diagram since the pedestrian flow increases even for high dense crowds. The reasons for this mismatching were studied through numerical computations and by a simple theoretical example. We arrived to the conclusion that either increasing the friction coefficient or increasing the relaxation time may be the key for achieving a non-increasing flow in the congested regime of the fundamental diagram. The second approach was already explored in Johansson (2009) and a similar idea was introduced in Parisi, 2009. We noticed, however, that both approaches are equivalent since both affect the reduced-in-units equation of motion in a similar fashion.

The analytical schematic model suggests that the problem could be addressed by modifying the friction coefficient. In light of this, we performed numerical simulations increasing κ and attained the fundamental diagram behavior reported in the empirical measurements.

When exploring the velocity profile, we found that it has a parabolic shape. Pedestrians reach the maximum velocity in the middle of the corridor while the minimum is by the walls. We found out that once scaled by v_{max} and the corridor width, the velocity profile yields a universal behavior (regardless the width of the corridor).

The phenomena reported in this paper suggests that further research needs to be done regarding the friction coefficient. We propose modeling the pedestrian-wall friction interaction with a different coefficient than the pedestrian-pedestrian friction interaction. We want to stress the fact that studying the friction coefficients may be a critical factor to properly reproduce the dynamics of a massive evacuation under high levels of anxiety.

6. Appendix: The reduced equation of motion

The equation of motion within the context of the Social Force Model includes at least six parameters (m , τ , A , B , κ and v_d), but the equation itself barely depends on two. The process of parameter's reduction is achieved by defining the (reduced) magnitudes

$$\begin{cases} t' &= t/\tau \\ r' &= r/B \\ v' &= v/v_d \end{cases} \quad (11)$$

The (reduced) equation of motion reads

$$\frac{d\mathbf{v}'}{dt'} = \frac{\tau}{m v_d} \left(\mathbf{f}_d + \mathbf{f}_s + \mathbf{f}_g \right) \quad (12)$$

It is straight forward from Eq. (12) that the corresponding reduced forces can be defined as follows

$$\begin{cases} \mathbf{f}'_d = \hat{\mathbf{e}}_d - \mathbf{v}' \\ \mathbf{f}'_s = \mathcal{A} \exp(r' - d') \hat{\mathbf{n}} \\ \mathbf{f}'_g = \mathcal{K} (2r' - d') \Theta(2r' - d') (\Delta \mathbf{v}' \cdot \hat{\mathbf{t}}), \hat{\mathbf{t}} \end{cases} \quad (13)$$

where $\mathcal{A} = A\tau/(m v_d)$ and $\mathcal{K} = \kappa B\tau/m$.

Notice that \mathcal{A} and \mathcal{K} are actually the only two control parameters in Eq. (12) for identical pedestrians. The ratio τ/m is common to both, but the magnitudes Av_d^{-1} and κB handle each parameter separately.

The fact that \mathcal{A} and \mathcal{K} share the parameter τ is in agreement with the conclusions outlined in Johansson (2009). The relaxation time (or “net-time headway”) τ actually “weights” the effects of the environment on the individual (that is, the social repulsion and the friction), and thus, appears as a “key control parameter” for the fundamental diagram as claimed in Johansson (2009).

The role of τ may be somewhat ambiguous whenever the social repulsion becomes negligible with respect to the friction. This may occur if some kind of balance exists between neighboring pedestrians in symmetrical configurations (*i.e.* in crowded corridors). We may hypothesize that the “key control parameter” may correspond to either τ , or, the friction itself κ . This is an open question, and a first order approach to this matter is outlined in Section 7.

7. A simple model for the corridor

A toy model for a moving crowd along a corridor is the one represented schematically in Fig. 8. Pedestrians (circles in Fig. 8) are assumed to be lined up from side to side across the corridor, at any given position. Social forces in the x -direction are further considered to vanish because of translational symmetry. Thus, only the sliding friction is allowed to balance the the pedestrians own desire. The (reduced) movement equation for the x -direction according to Section 6 and Fig. 8 is

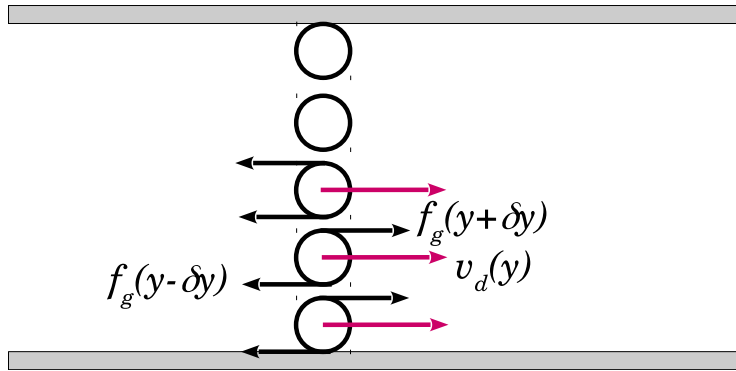


Figure 8: Schematic diagram for individuals in a corridor. The circles represent pedestrians moving from left to right. The desired force (red arrows) and sliding friction (black arrows) are assumed to be the only relevant forces.

$$\frac{dv'}{dt'}(y') = 1 - v'(y') + f'_g(y' + \delta y') - f'_g(y' - \delta y') \quad (14)$$

where $v'(y')$ corresponds to the (reduced) velocity (for the x -direction) of the individual located at the y' position. Notice that the individuals remain at the same y' position while traveling through the corridor, since balance is expected to take place across the corridor. These positions are roughly $\delta y'$, $3\delta y'$, $5\delta y'$, Actually, it is not relevant (for now) the value of y' , and a further simplification can be done by labeling $v'(y') = v_i$ and $v'(y' \pm 2\delta y') = v_{i\pm 1}$. The velocity of the individual in contact with the bottom wall in Fig. 8 will be labeled as v_1 .

The last two terms in Eq. (14) correspond to the net drag applied on the pedestrian with velocity v_i . According to Eq. (13) this drag may be expressed as

$$f'_{g,i+\frac{1}{2}} - f'_{g,i-\frac{1}{2}} = \begin{cases} 2\alpha v_2 - 3\alpha v_1 & i = 1 \\ 2\alpha (v_{i+1} - 2v_i + v_{i-1}) & i > 1 \end{cases} \quad (15)$$

for $\alpha = \mathcal{K}(r' - \delta y')$. Recall that our first order approach considers $\delta y'$ as roughly uniform across the corridor.

The stationary situation can be computed straight forward from Eq. (14). Thus, for $\dot{v}_i = 0$ the following set of equations determine the velocity profile in the corridor (within this toy model)

$$\begin{cases} (3\alpha + 1) v_1 - 2\alpha v_2 & = 1 \\ -2\alpha v_{i-1} + (4\alpha + 1) v_i - 2\alpha v_{i+1} & = 1 \end{cases} \quad (16)$$

Notice from Eq. (15) that $\alpha = 0$ means no friction at all, and thus, the individuals are allowed to move free from drag. It can be verified that $v_i = 1$ solves the set (16) for this scenario. The $\alpha = 0$ scenario is expected to occur, however, for densities below a contacting threshold.

A boundary condition needs to be imposed in order to solve Eqs. (16) for $\alpha \neq 0$. We fix $v_i = v_{i+1}$ at the middle of the corridor since the velocity profile should be specularly distributed with respect to the mid-axis of the corridor. Fig. 9 shows the computed mean velocity for the bottom side profile as function of α .

Fig. 9 exhibits a decreasing behavior for increasing values of α . As explained above, the maximum value occurs at $\alpha = 0$ (*i.e.* $\langle v_i \rangle = 1$). However, the decreasing slope slows down for increasing number of individuals. This corresponds to a flattening in the velocity profile, (see Section 4 for details).

The mean flux of individuals can be built from the mean velocity and the corresponding pedestrian density as follows

$$J = \begin{cases} \rho & \text{for } \alpha = 0 \\ (\rho_0 + c\alpha) \langle v_i \rangle & \text{for } \alpha > 0 \end{cases} \quad (17)$$

where $\langle v_i \rangle$ equals unity for the case $\alpha = 0$, and thus, it was omitted in (17). The density $\rho = \rho_0 + c\alpha$ corresponds to the packing density (that is, the density above the contacting

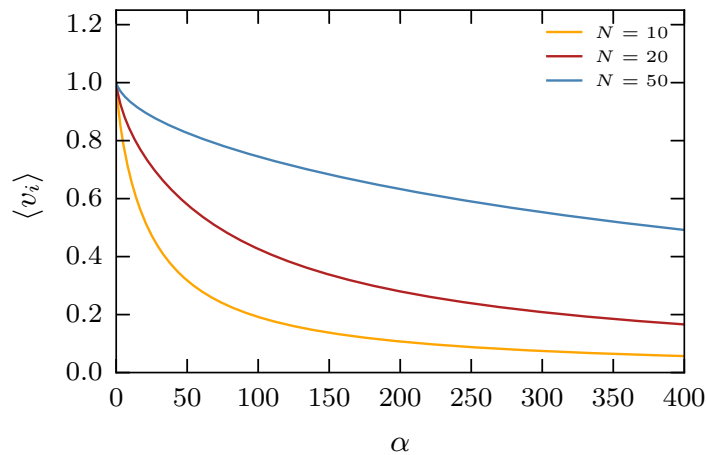


Figure 9: Mean velocity of the bottom half of the individuals vs. the parameter α . Both axis are dimensionless. N corresponds to the number of individuals.

threshold) and c corresponds to a somewhat “packing coefficient”. Fig. 10 shows the flow as a function of the density, assuming $\rho_0 = 1$ for simplicity.

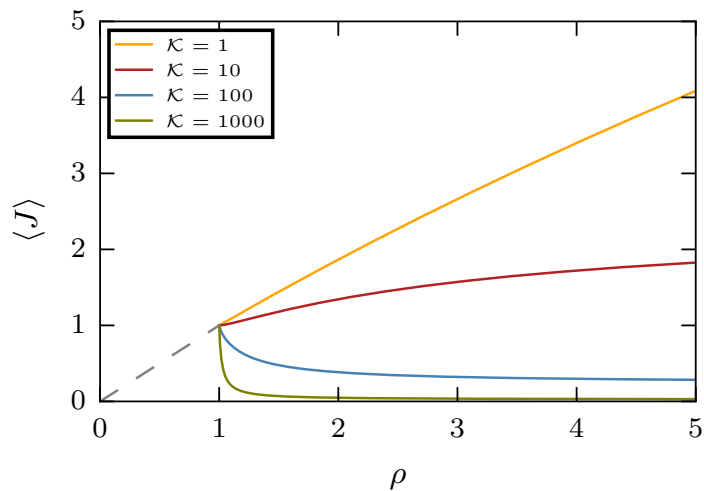


Figure 10: Mean flux of the bottom half of the individuals vs. the pedestrian (global) density ρ (see text for details). Both axis are dimensionless. The number of individuals across the corridor was set to $N = 10$, and the contacting threshold was set to $\rho_0 = 1$. The “packing coefficient” was set to $c = 1/\mathcal{K}$ (and thus, making the term $c\alpha$ independent of friction). The dashed line corresponds to the flux at the low density regime (say, $\langle v_i \rangle = 1$).

The pedestrian flux J attains two possible behaviors, according to Fig. 10. For packing coefficients $c < 0.05$, the flux diminishes as the corridor becomes more crowded. But, if c surpasses this threshold, the flux slope becomes positive, although the mean velocity diminishes. We conclude that the role of the pedestrians’ friction coefficient is crucial for building the fundamental diagram.

REFERENCES

- A. Colombi, M. Scianna, and A. Alaia, *Computational and Applied Mathematics* 36, 1113 (2017)
- G. Frank and C. O. Dorso, *Physica A* 390, 2135 (2011).
- D. Helbing and P. Molnr, *Physical Review E* 51, 4282 (1995).
- D. Helbing, I. Farkas, and T. Vicsek, *Nature* 407, 487 (2000).
- D. Helbing, A. Johansson, and H. Z. Al-Abideen, *Physical review E* 75, 046109 (2007).
- A. Johansson, D. Helbing, and P. K. Shukla, *Advances in Complex Systems* 10, 271 (2007).
- A. Johansson, *Phys. Rev. E* 80, 026120 (2009).
- J. Kwak, H.-H. Jo, T. Lutinen, and I. Kosonen, *Physical Review E* 96, 022319 (2017).
- T. I. Lakoba, D. J. Kaup, and N. M. Finkelstein, *Simulation* 81, 339 (2005).
- D. Parisi and C. O. Dorso, *Physica A* 354, 606 (2005).
- D. Parisi and C. O. Dorso, *Physica A* 385, 343 (2007).
- D. R. Parisi, M. Gilman, and H. Moldovan, *Physica A: Statistical Mechanics and its Applications* 388, 3600 (2009).
- A. Seyfried, B. Steffen, W. Klingsch, and M. Boltes, *Journal of Statistical Mechanics: Theory and Experiment* 2005, P10002 (2005).
- A. Seyfried, B. Steffen, and T. Lippert, *Physica A: Statistical Mechanics and its Applications* 368, 232 (2006).
- A. Seyfried, M. Boltes, J. Khler, W. Klingsch, A. Portz, T. Rupprecht, A. Schadschneider, B. Steffen, and A. Winkens, in *Pedestrian and Evacuation Dynamics 2008*, edited by W. W. F. Klingsch, C. Rogsch, A. Schadschneider, and M. Schreckenberg (Springer Berlin Heidelberg, Berlin, Heidelberg, 2010) pp. 145-156.
- Plimpton S. (1995), "Fast parallel algorithms for short-range molecular dynamics", *Journal of Computational Physics*, 117, 1, 1–19.
- I. Sticco, G. Frank, S. Cerrotta, and C. Dorso, *Physica A: Statistical Mechanics and its Applications* 474, 172 (2017).
- I. Sticco, F. Cornes, G. Frank, and C. Dorso, *Physical Review E* 96, 052303 (2017).